

Numerical simulation of excitation and propagation of helioseismic MHD waves in magnetostatic models of sunspots

K. Parchevsky, A. Kosovichev¹, E. Khomenko^{2,3}, V. Olshevsky³, M. Collados²

Stanford University, HEPL, Stanford CA 94305, USA

kparchevsky@solar.stanford.edu

ABSTRACT

We present comparison of numerical simulations of propagation of MHD waves, excited by subphotospheric perturbations, in two different ("deep" and "shallow") magnetostatic models of the sunspots. The "deep" sunspot model distorts both the shape of the wavefront and its amplitude stronger than the "shallow" model. For both sunspot models, the surface gravity waves (f -mode) are affected by the sunspots stronger than the acoustic p -modes. The wave amplitude inside the sunspot depends on the photospheric strength of the magnetic field and the distance of the source from the sunspot axis. For the source located at 9 Mm from the center of the sunspot, the wave amplitude increases when the wavefront passes through the central part of the sunspot. For the source distance of 12 Mm, the wave amplitude inside the sunspot is always smaller than outside. For the same source distance from the sunspot center but for the models with different strength of the magnetic field, the wave amplitude inside the sunspot increases with the strength of the magnetic field. The simulations show that unlike the case of the uniform inclined background magnetic field, the p - and f -mode waves are not spatially separated inside the sunspot where the magnetic field is strongly non-uniform. These properties have to be taken into account for interpretation of observations of MHD waves traveling through sunspot regions.

Subject headings: Sun: oscillations—sunspots

¹Stanford University, HEPL, Stanford CA 94305, USA.

²Instituto de Astrofísica de Canarias, 38205, C/Vía Láctea, s/n, Tenerife, Spain.

³Main Astronomical Observatory, NAS, 03680 Kyiv, Ukraine.

1. Introduction

Details of MHD wave propagation inside magnetized regions are very important for understanding of interaction, scattering, and conversion of seismic waves by sunspots in the Sun. The structure of sunspots themselves is not well understood. Pizzo (1986) proposed a self-consistent magnetostatic sunspot model. Later Low (1975) presented a self-similar model. These two models (model of Pizzo at the top and model of Low at the bottom) were joined by Khomenko & Collados (2008). It is well understood now that the sunspot is dynamic, so several attempts have been made to build numerically a stable sunspot model with the background flows (Hurlburt & Rucklidge 2000; Botha et al. 2008). Recently Rempel et al. (2009) obtained realistically looking penumbral structures with outflows.

Local helioseismology provides a tool for reconstruction of the internal structure (both profiles of wave speed and flows) of sunspots from Doppler observations. The magnetic field of sunspots affect the result of the helioseismic inversion. For understanding the helioseismic effects of the magnetic field it is important to perform direct simulations of MHD waves in different models of sunspots. The simulations are also used for producing artificial data for calibration and testing of helioseismic measurements and inversion algorithms. There is wide gallery of numerical simulations of propagation of MHD waves inside sunspots illustrating various observed phenomena: power deficit of p -modes, acoustic halos, azimuthal phase shift variations of the signal in the sunspot penumbra, and so on. Not all of these phenomena are caused by the direct effects of magnetic fields. Indirect effects of magnetic fields must be also taken into account. For instance, Parchevsky & Kosovichev (2007b) showed that 50% of the observed acoustic power deficit in sunspots can be explained by the absence of the acoustic sources inside sunspots, where strong magnetic field inhibits convective motions, which are the primary source of solar oscillations. The suppression of acoustic sources is one of the most important indirect effects of the solar magnetoseismology. Another example of the indirect effects are changes in the density and temperature stratifications caused by magnetic fields. Among the direct effects of magnetic field (effects caused by magnetic stresses on wave perturbations) an important role is played by conversion into different types of MHD waves. For instance, 2D simulations of wave propagation in inclined magnetic fields (e.g Cally & Bogdan (1997); Cally (2000); Spruit & Bogdan (1992)) showed that fast MHD waves can be converted into slow MHD waves, which can leave the computational domain, and thus interpreted as an "absorption" of the fast mode. Acoustic halos around sunspots were obtained in simulations by Hanasoge (2008) as a result of wave transformations. However, Jacoutot et al. (2008) noted that this effect can be explained by changes in the excitation properties of solar convection in moderate field strength regions. Cameron et al. (2008) obtained the peak restrictions of 3 kG for the photospheric magnetic field strength from simulations of scattering f -modes by the sunspot. Three dimensional simulations of

linear MHD wave propagation performed by Parchevsky & Kosovichev (2009) show that the inclined magnetic field can be partly responsible for the azimuthal variations of travel times around sunspots found by Zhao & Kosovichev (2006) from helioseismic observations. Refraction of upward propagating MHD waves in the solar atmosphere was simulated by e.g. Khomenko & Collados (2006); Cally & Goossens (2008). Recently, Khomenko et al. (2009) carried out 2D simulations of the interaction of MHD waves with magnetostatic sunspot models. In this paper we present initial results of our 3D modeling of this problem.

Results of linear numerical simulations of MHD waves propagation in sunspots mainly depend on the setup of the problem: 2D or 3D simulations, choice of the background model of the sunspot, the way of excitation of the waves, and treating of the boundary conditions. The goal of this paper is to study and compare properties of 3D propagation of MHD waves in different magnetostatic models of sunspots, and also describe how different types of waves are affected by the sunspot. Waves are generated by localized subphotospheric (depth of 100 km) sources of the vertical force. For such sources simulated waves propagate along the same ray paths as in the Sun. The numerical method and the background sunspot models are described in §2 and §3. The results of simulations are discussed in §4.

2. Governing equations

Propagation of MHD waves inside the Sun is described by the following system of linearized equations:

$$\begin{aligned}
 \frac{\partial \rho'}{\partial t} + \nabla \cdot \mathbf{m}' &= 0, \\
 \frac{\partial \mathbf{m}'}{\partial t} + \nabla p' - \frac{1}{4\pi} [(\nabla \times \mathbf{B}') \times \mathbf{B}_0 + (\nabla \times \mathbf{B}_0) \times \mathbf{B}'] &= \rho' \mathbf{g}_0 + \mathbf{S}(r, t), \\
 \frac{\partial \mathbf{B}'}{\partial t} &= \nabla \times \left(\frac{\mathbf{m}'}{\rho_0} \times \mathbf{B}_0 \right), \\
 \frac{\partial p'}{\partial t} + c_{s0}^2 \nabla \cdot \mathbf{m}' + c_{s0}^2 \frac{\mathcal{N}_0^2}{g_0} m_z &= 0,
 \end{aligned} \tag{1}$$

where $\mathbf{m}' = \rho_0 \mathbf{v}'$ is the momentum perturbation, \mathbf{v}' , ρ' , p' , and \mathbf{B}' are the velocity, density, pressure, and magnetic field perturbations respectively, $\mathbf{S}(r, t) = (0, 0, S_z(r, t))^T$ is the wave source function. The quantities with subscript 0, such as gravity \mathbf{g}_0 , sound speed c_{s0} , and Brünt-Väisälä frequency \mathcal{N}_0 correspond to the background model, \mathbf{B}_0 is the background magnetic field satisfying the usual magnetohydrostatic equilibrium equation. The spatial

and temporal behavior of the wave source is modeled by function $S_z(r, t) = AH(r)F(t)$:

$$H(r) = \begin{cases} \left(1 - \frac{r^2}{R_{src}^2}\right)^2 & \text{if } r \leq R_{src} \\ 0 & \text{if } r > R_{src} \end{cases} \quad (2)$$

$$F(t) = (1 - 2\tau^2) e^{-\tau^2}. \quad (3)$$

where R_{src} is the source radius, $r = \sqrt{(x - x_{src})^2 + (y - y_{src})^2 + (z - z_{src})^2}$ is the distance from the source center, τ is given by equation

$$\tau = \frac{\omega_0(t - t_0)}{2} - \pi, \quad t_0 \leq t \leq t_0 + \frac{4\pi}{\omega}, \quad (4)$$

where ω_0 is the central source frequency, t_0 is the moment of the source initiation. This source model provides the wave spectrum, which closely resembles the solar spectrum. It has a peak near the central frequency ω_0 and spreads over a broad frequency interval. The source spectrum is:

$$|\hat{F}(\omega)| \equiv \left| \int_{-\infty}^{\infty} F(t) e^{-i\omega t} dt \right| = 4\sqrt{\pi} \frac{\omega^2}{\omega_0^3} e^{-\frac{\omega^2}{\omega_0^2}}. \quad (5)$$

A superposition of such sources with uniform distribution of central frequencies randomly distributed below the photosphere describes very well the observed solar oscillation spectrum (Parchevsky & Kosovichev 2007a).

For numerical solution of Eqs (1) a semi-discrete finite difference scheme of high order was used. At the top and bottom boundaries non-reflective boundary conditions based on the Perfectly Matched Layer (PML) technique were set. Details of numerical realization of the code can be found in Parchevsky & Kosovichev (2007a).

3. Background model of the sunspot

We used two types of axially symmetric magnetohydrostatic background models of the sunspot described in Khomenko & Collados (2008) ("shallow" model) and Khomenko & Collados (2005) ("deep" model). The "shallow" sunspot model is obtained as a combination of the self-similar solution (Low 1975) in deep layers with the solution of Pizzo (Pizzo 1986) in upper layers. We calculated three instances (a), (b), and (c) of the "shallow" model with the following photospheric strengths of the magnetic field at the sunspot axis: 0.83 kG, 1.4 kG, and 2.2 kG respectively. Strengths of the magnetic field at the bottom of the domain for these models are 5.0 kG, 8.0 kG, and 12.5 kG respectively. The depth of the domain (from the photosphere) for the "shallow" models is 9.87 Mm. The position of the photosphere

for the "quiet" Sun (at the boundary of the sunspot) coincides with the photospheric level in the standard model S (Christensen-Dalsgaard et al. 1996). For comparison purposes we calculated one instance of the "deep" sunspot model with the maximum strength of the magnetic field of 843 G at the photosphere and 29 kG at the bottom of the domain. The "deep" sunspot model is based on solution of Pizzo everywhere in the domain. The depths of the deep model is 7.5 Mm.

Maps of the relative sound speed perturbations for the "shallow" (panel a) and "deep" (panel c) models with photospheric strength of the magnetic field of 843 G and 836 G respectively are presented in Figure 1. The black horizontal line marks the position of the photosphere. The red curve shows position of $\beta = 1$ level. Both types of the models were calculated under the assumption that $\Gamma_1 = 5/3$. Panels b and d show variations of relative speed of the fast MHD wave. The velocity of the fast MHD wave depends on the angle between the wave vector and the vector of the magnetic field. The maximum value is plotted. So, panels (a) and (b) represent bottom and top limits (depending on the direction of propagation) for the speed of the fast MHD wave for the "shallow" model. Panels (c) and (d) represent speed limits for the "deep" model.

There are three main differences between these models: (i) the topology of the magnetic field, (ii) the strength of the magnetic field near the bottom of the domain, and (iii) dependence of the horizontal profile of the sound speed on the depth. The magnetic field lines (shown by blue curves in both panels of Figure 1) are convex near the photosphere for the "deep" model while in the "shallow" model the field lines are concave near the photosphere. One dimensional cuts of the horizontal profiles of the sound speed for different depths are shown in Figure 2. Profiles are scaled by the sound speed c_{quiet} taken at the same depth of the outer boundary of the sunspot. In the "shallow" model sound speed perturbation $\delta c/c = c/c_{quiet} - 1$ is close to zero everywhere starting from the depth of about 2 Mm. In the "deep" model the sound speed perturbation is non zero even at the bottom of the domain at 7.5 Mm. This means, that in the "shallow" model waves, propagating at distances greater than 10 Mm, propagate mostly in the region with the sound speed profile of the quiet Sun below the region with the perturbed sound speed. The vertical sound speed profiles at the sunspot center and at the boundary for both models are shown in Figure 3.

The sound speed profiles along with the magnetic field structure are the most significant parameters affecting propagation of the MHD waves through the sunspot.

4. Results and discussion

In this section we present results of simulation of MHD waves generated by a single source in different magnetohydrostatic self-consistent background models. Axially symmetric models of sunspots were interpolated on Cartesian grid with $\Delta x = \Delta y = 0.15$ Mm. Vertical grid is non-uniform. We have three instances (a), (b), and (c) of the "shallow" model (discussed above) with the grid size of $376 \times 376 \times 67$ and depth of 9.87 Mm (from the photosphere). The vertical z-grid step varies from $\Delta z = 0.05$ Mm at the level of the photosphere and above to $\Delta z = 0.52$ Mm at the bottom of the domain. Time step $\Delta t = 0.05$ s is the same for simulations with all three instances of the background "shallow" model. The "deep" model has the grid size of $184 \times 184 \times 62$, depth of 7.5 Mm (from the photosphere), and $\Delta t = 0.1$ s. The vertical z-grid step varies from $\Delta z = 0.05$ Mm at the level of the photosphere and above to $\Delta z = 0.4$ Mm at the bottom of the domain.

The source of the vertical component of force described above with the spectrum given by Eq. (5) is placed at the distance of 9 Mm from the axis of the sunspot for the "shallow" models and 6 Mm for the "deep" model. The depth of the source is 0.1 Mm for both models. The top absorbing PML is placed at the height of 0.5 Mm and extends up to 0.9 Mm. In this region the vertical profile of the sound speed at the outer boundary of the sunspot is close to the profile in the standard solar model with $\Gamma_1 = 5/3$. The lateral boundary conditions are chosen to be periodic.

Snapshots of the simulated wavefield for the "deep" model are shown in Figure 4. Panels a, b, and c represent maps of perturbations of density ρ' , z-momentum $\rho_0 w'$, and vertical component of the magnetic field B'_z respectively at moment $t = 20$ min. Panels d, e, and f represent maps of the same variables at $t = 25$ min. Each panel consists of horizontal XY-slice at the photospheric level (top) and vertical XZ-slice through the center of the sunspot (bottom). The white line in the XZ-slice shows position of the photosphere. Solid black curves represent the magnetic field lines. The dashed lines near the top and bottom of the XZ-slice show the position of the damping layers. For the reference we plotted a circle with radius of 5 Mm and origin at the wave source location. The non-uniform background model causes anisotropy of the amplitude of the wave front. When the wave front reaches the center of the sunspot the amplitude of density and momentum perturbations decrease. After passing the center of the sunspot the amplitude restores its original value. At some moments, the amplitude inside the sunspot can become greater than the amplitude of wave propagating outside the sunspot. The shape of the wave front is changed as well. This is more noticeable for inner parts of the wave front, located inside the circle in panels a, b, and c. Later we show that these parts of the wave front are formed mostly by f -modes. The shape of the outer parts of the wave front (formed mostly by p -modes) remains close to the

circle. A wave, propagating along the magnetic field lines is appeared at the source location. It is clearly seen in vertical slices of $\rho_0 w'$ and B'_z , but absent in ρ' . This wave consists of a mixture of the Alfvén and slow MHD waves.

It is interesting to compare propagation of MHD waves in the "deep" and "shallow" models with similar photospheric strength of the magnetic field. Results of wave simulations in the "shallow" model with the photospheric strength of the magnetic field $B_0 = 0.83$ kG are shown in Figure 5. There are common features with simulations for the "deep" model and there are differences. In general, in the "shallow" model waves show the same behavior as in the "deep" model. The amplitude of ρ' and $\rho_0 w'$ decreases when the wave front reaches the center of the sunspot, but the ratio of amplitudes is closer to unity than in the "deep" model. After passing the center of the sunspot the wave restores its amplitude. The amplitude of momentum perturbations $\rho_0 w'$ becomes slightly bigger inside the sunspot than outside, but again, not as much as in the "deep" model. Perturbation of density ρ' remains smaller inside the sunspot than outside for all moments of time. The wave that contains a mixture of the Alfvén and slow MHD waves is generated near the source location, as in the "deep" model, but the amplitude of this wave is much smaller and it is not seen in Figure 5. The shape of the wave front is more circular than in simulations for the "deep" model. In general, we can say, that the "shallow" model affects the waves less than the "deep" model.

Comparison of the z-momentum maps at the same moments of time in different instances of the "shallow" model with different strength of the photospheric magnetic field is shown in Figure 6. The wave amplitude inside the sunspot grows with the strength of the magnetic field and for the surface strength of 2.2 kG the wave amplitude inside the sunspot becomes bigger than outside.

Behavior of MHD waves inside sunspots depends on the distance of the wave source from the sunspot center. This happens because magnetoacoustic waves in the Sun propagate through the solar interior. This means that waves, generated by the source located farther from the sunspot center, propagate deeper (in the region with stronger magnetic field) than waves from the closer source. The angle between the direction of wave propagation and the background magnetic field is also different in these two cases. Snapshots of the wave field for the "shallow" model with surface strength of the magnetic field 2.2 kG are shown in Figure 7. The left panel represents the wave generated by the source located at 9 Mm from the sunspot axis. In the right panel the source is located at 12 Mm from the sunspot center. The wave amplitude from the close source at some moment of time becomes bigger inside the sunspot than outside. The amplitude of the wave front of the distant source remains smaller inside the sunspot than outside for all moments of time.

The wave source generates a mixture of fast, slow, Alfvén, and magnetogravity waves.

The spectrum ($k - \nu$ diagram) for this case is shown in Figure 8. The solid black curve represents the theoretical curve of the f -mode in absence of the magnetic field. The fast MHD and magnetogravity modes can be separated by filtering out the f -mode. Result of such separation is shown in Figure 9. The top row represents the original k - ν diagram (obtained from the z -component of velocity at the photospheric level) and k - ν diagrams obtained by filtering out f - and p -modes respectively. The white solid curve shows the theoretical position of the f -mode ridge in the absence of the magnetic field. The middle row represents maps of V_z for p - and f -modes at the photospheric level at the moment $t=23$ min. It was shown (Parchevsky & Kosovichev 2009) that in case of the horizontally uniform background model and uniform inclined background magnetic field wavefronts of p - and f -modes are spatially separated after 20-30 min. This does not happen in the case of the non-uniform background magnitohydrostatic model. The solid black circle marks the inner part of the wavefront of p -modes. Although the amplitude of the f -modes (the right panel) is mostly concentrated inside the circle, there is noticeable non-zero amplitude in the region outside the circle where p -modes present. It is clear, that the deformation of the wavefront (both the shape and wave amplitude) due to the interaction with the sunspot is much stronger for f -modes than for p -modes. The wave amplitude of the p -mode wavefront decreases at the sunspot center and quickly restores its value when the front passes through the center. The amplitude of the f -mode wavefront remains perturbed at all moments of time.

5. Conclusion

According to our 3D numerical simulations of MHD wave propagation in two different models (referred as "shallow" and "deep") we can point out to the following characteristic behavior of waves inside sunspots. The interaction with the sunspot changes the shape of the wave front and amplitude of the f -mode waves significantly stronger than of the p -mode waves. The amplitude of the wave front of the p -modes decreases when the wave reaches the sunspot center and restores its original value when the wave passes the center of the sunspot. The "shallow" model of sunspot affects waves less than the "deep" model. This means that the horizontal inhomogeneity of the sound speed profile inside the sunspot is mostly responsible for perturbations of the wave front. In the "shallow" model the horizontal distribution of the sound speed below 2 Mm is almost uniform and the sound speed coincides with the value in the quiet Sun at the same depth. Only magnetic field perturbs the wave front in this region and the total perturbation of the wave front becomes weaker than in the "deep" case.

Inside the sunspot magnetoacoustic and magnetogravity waves are not spatially separated unlike the case of the uniform inclined magnetic field. The wave amplitude inside sunspots depends on the strength of the magnetic field and the distance of the wave source from the sunspot axis. The stronger photospheric magnetic field, the bigger wave amplitude inside the sunspot (if the source is located at the same distance from the sunspot center). For the source located at 9 Mm from the sunspot axis the wave amplitude inside the sunspot at some moment becomes bigger than the amplitude outside. For the source located at 12 Mm the wave amplitude inside the sunspot remains smaller than outside for all moments of time.

In this paper, we presented initial results of 3D simulations of helioseismic MHD waves in magnetostatic sunspot models. Future work includes simulations with multiple random sources for testing the travel-time measurement procedures of time-distance helioseismology, and also modeling wave propagation in the MHD models of sunspots, including flows (Botha et al. 2008; Hurlburt & Rucklidge 2000).

REFERENCES

- Botha, G.J.J., Busse, F.H., Hurlburt, N.E., and Rucklidge, A.M. 2008, *MNRAS*, 387, 1445
- Cally, P.S. and Bogdan, T.J. 1997, *ApJ*, 486, L67
- Cally, P. 2000, *Solar Phys.*, 192, 395
- Cally, P. and Goossens, M. 2008, *Solar Phys.*, 251, 251
- Cameron, R., Gizon, L., and Duvall Jr., T.L. 2008, *Solar Phys.*, 251, 291
- Christensen-Dalsgaard, J., et al. 1996, *Science*, 272, 1286
- Hanasoge, S.M. 2008, *ApJ*, 680, 1457
- Hurlburt, N.E. and Rucklidge, A.M. 2000, *MNRAS*, 314, 793
- Jacoutot, L., Kosovichev, A.G., Wray, A., and Mansour, N.N. 2008, *ApJ*, 684, L51
- Khomenko, E., Kosovichev, A., Collados, M., Parchevsky, K., and Olshevsky, V. 2009, *ApJ*, 694, 411
- Khomenko, E., & Collados, M. Proceedings of the International Scientific Conference on Chromospheric and Coronal Magnetic Fields (ESA SP-596). 30 August - 2 September

- 2005, Katlenburg-Lindau, Germany. Editors: D.E. Innes, A. Lagg & S.K. Solanki, Published on CDROM, p.40.1
- Khomenko, E., and Collados, M. 2006, ApJ, 653, 739
- Khomenko, E., & Collados, M. 2008, ApJ, 689, 1379
- Low, B.C. 1975, ApJ, 197, 251
- Parchevsky, K. V. and Kosovichev, A. G. 2007a, ApJ, 666, 547
- Parchevsky, K. V. and Kosovichev, A. G. 2007b, ApJ, 666, L53
- Parchevsky, K. V. and Kosovichev, A. G. 2009, ApJ, 694, 573
- Pizzo, V.J. 1986, ApJ, 302, 785
- Rempel, M., Schussler, M., Cameron, R.H., Knolker, M. 2009, Science, 325, 171
- Spruit, H.C. and Bogdan, T.J. 1992, ApJ, 391, L109
- Zhao, J. and Kosovichev, A., G. 2006, ApJ, 643, 1317.

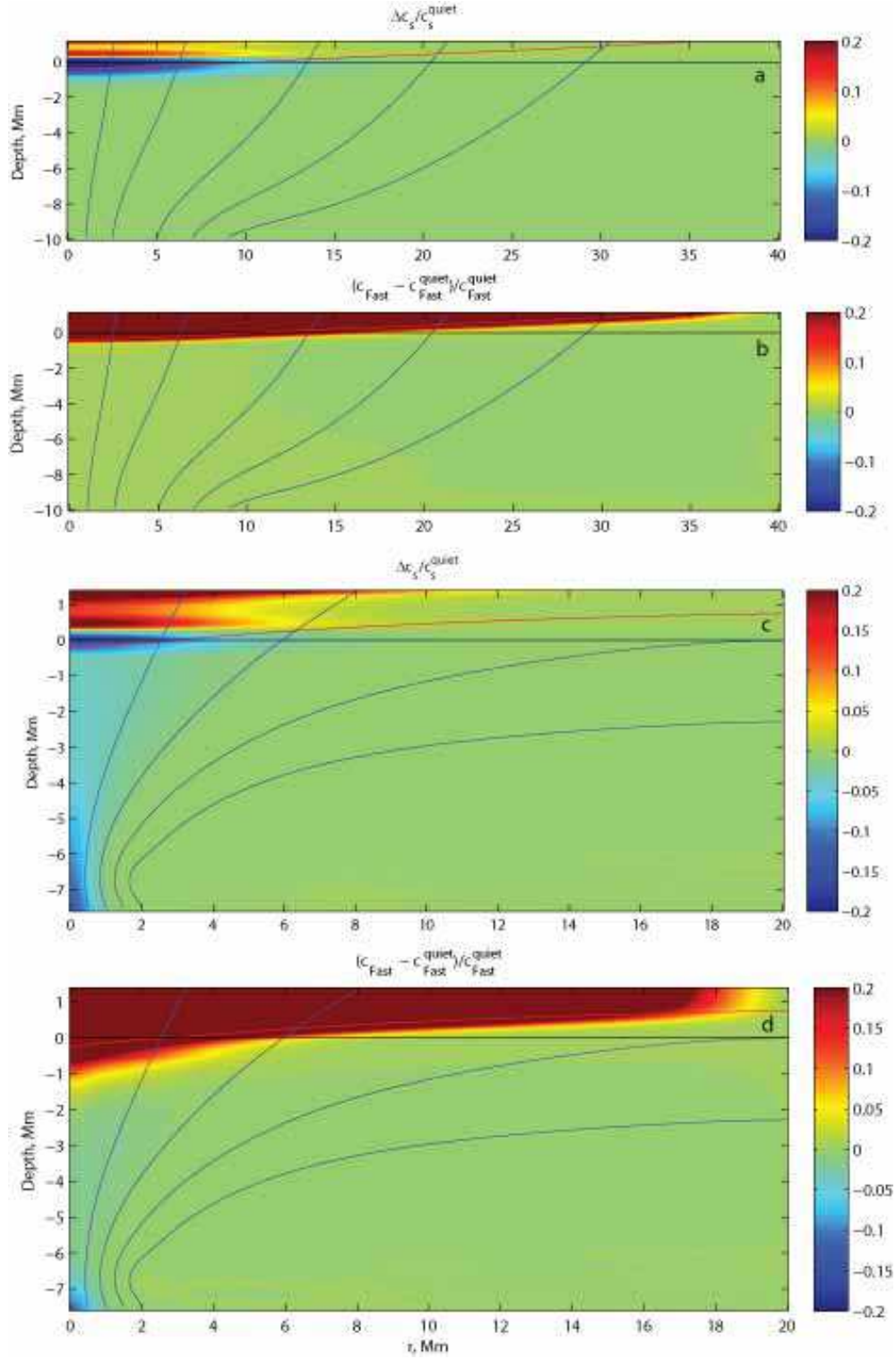


Fig. 1.— Maps of the relative sound speed perturbation $\Delta c/c$ in the "shallow" (panel a) and the "deep" (panel c) sunspot models. Panels (b) and (d) show maps of relative speed perturbations of fast MHD waves for the "shallow" and "deep" models respectively. The solid horizontal black line and the red curve represent the level of the photosphere of the quiet Sun and level $\beta = 1$ respectively.

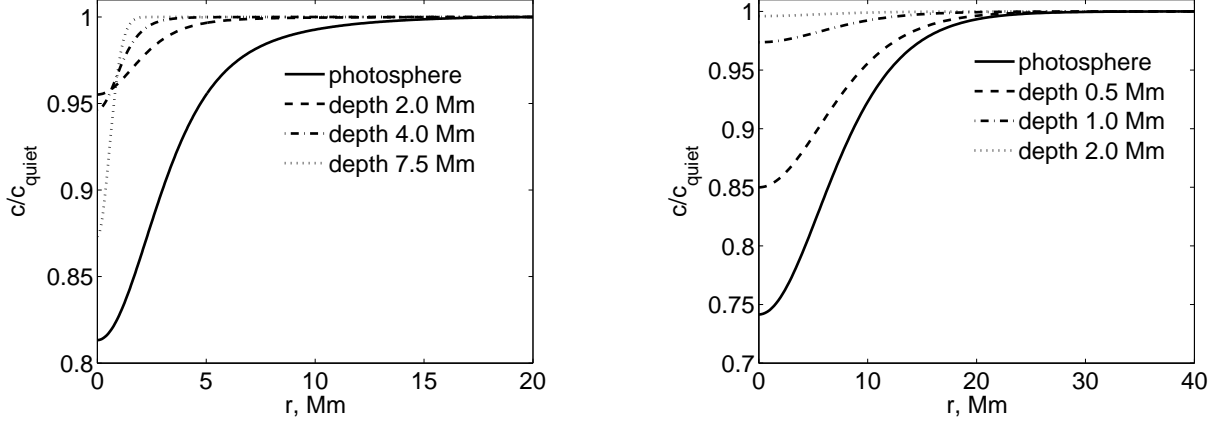


Fig. 2.— Perturbations of the sound speed for different depth for the "deep" model (left panel) and the "shallow" model (right panel). For the "shallow" model horizontal variations of the sound speed is negligible below 2 Mm.

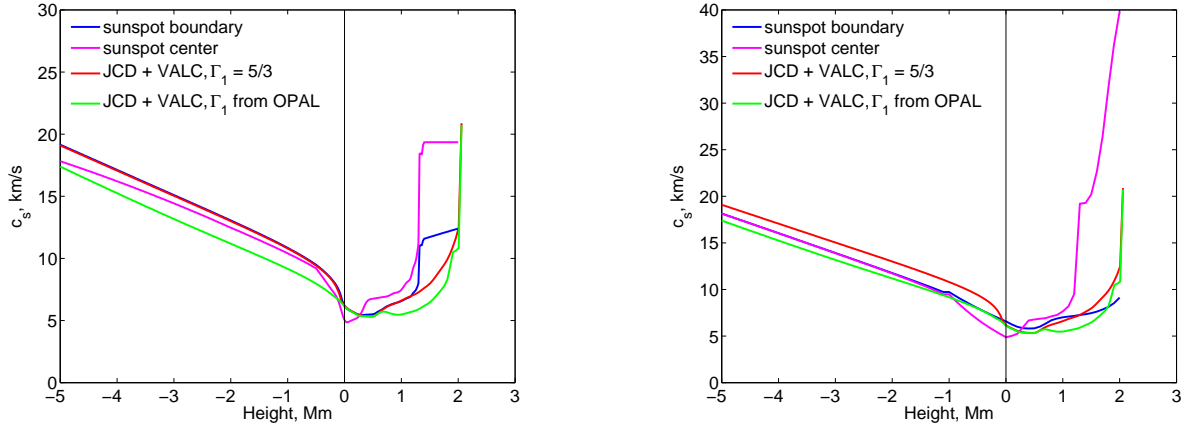


Fig. 3.— Vertical profiles of perturbations of the sound speed for the "deep" (left) and the "shallow" (right) sunspot models. The magenta curve represents the vertical profile at the sunspot center. The blue curve shows the sound speed profile at the sunspot boundary. For comparison we plotted the sound speed profile from the standard solar model S by Christensen-Dalsgaard with smoothly joined VALC model of the chromosphere (green). Adiabatic exponent Γ_1 is calculated from the OPAL equation of state. The same curve, but with $\Gamma_1 = 5/3$ is shown by red color.

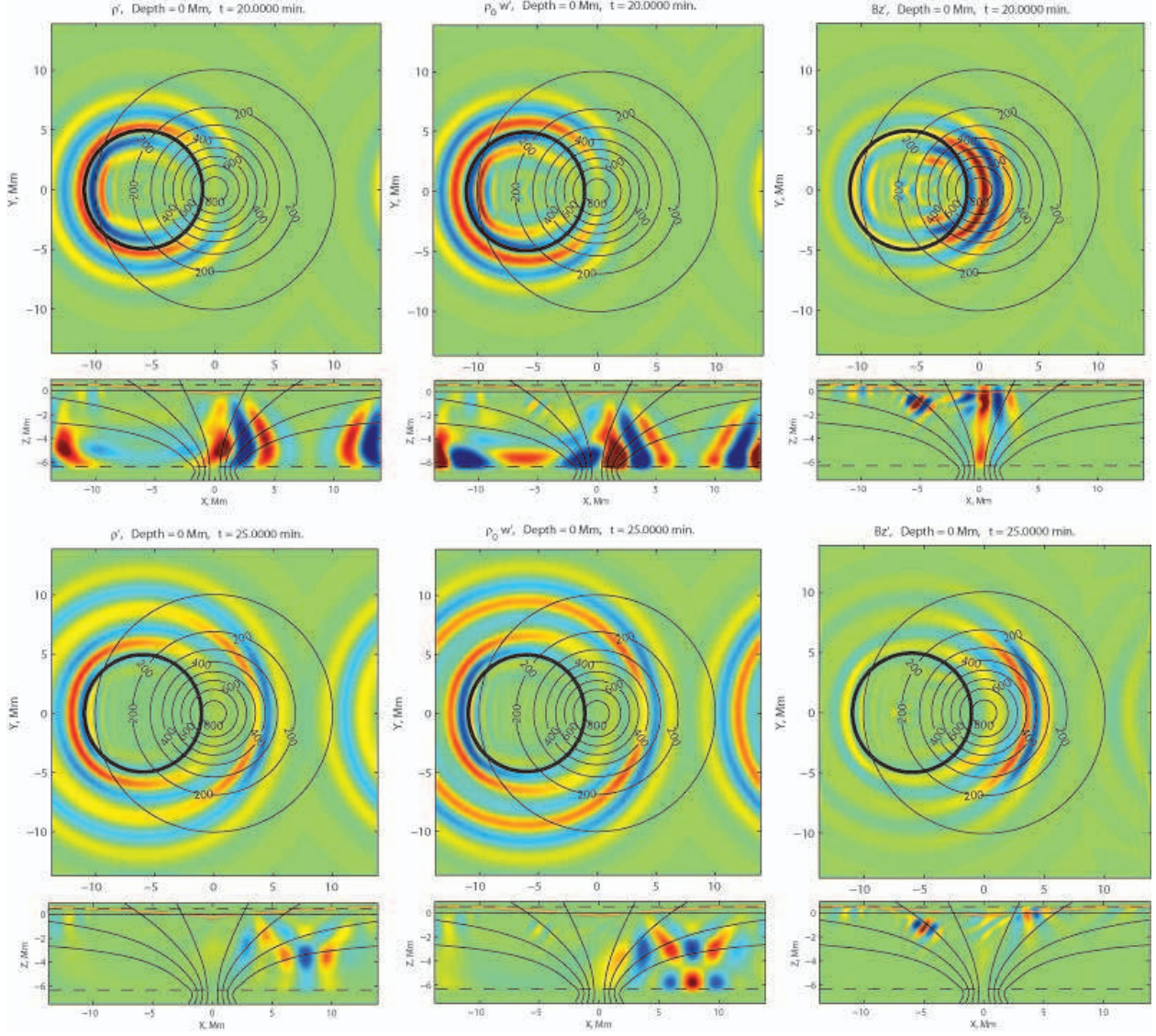


Fig. 4.— Snapshot of density ρ' (left), z-momentum $\rho_0 w'$ (middle), and B'_z (right) perturbations in the wave, propagating in the "deep" model, at moments $t=20$ min. (top) and $t = 25$ min. (bottom). Each panel consists of two pictures: the horizontal slice of the domain at the photospheric level (top) and vertical cuts of the domain (bottom). The solid black horizontal lines and red curves in the vertical cuts represent the position of the quiet photosphere and the level $\beta = 1$ respectively. Solid black curves represent the magnetic field lines.

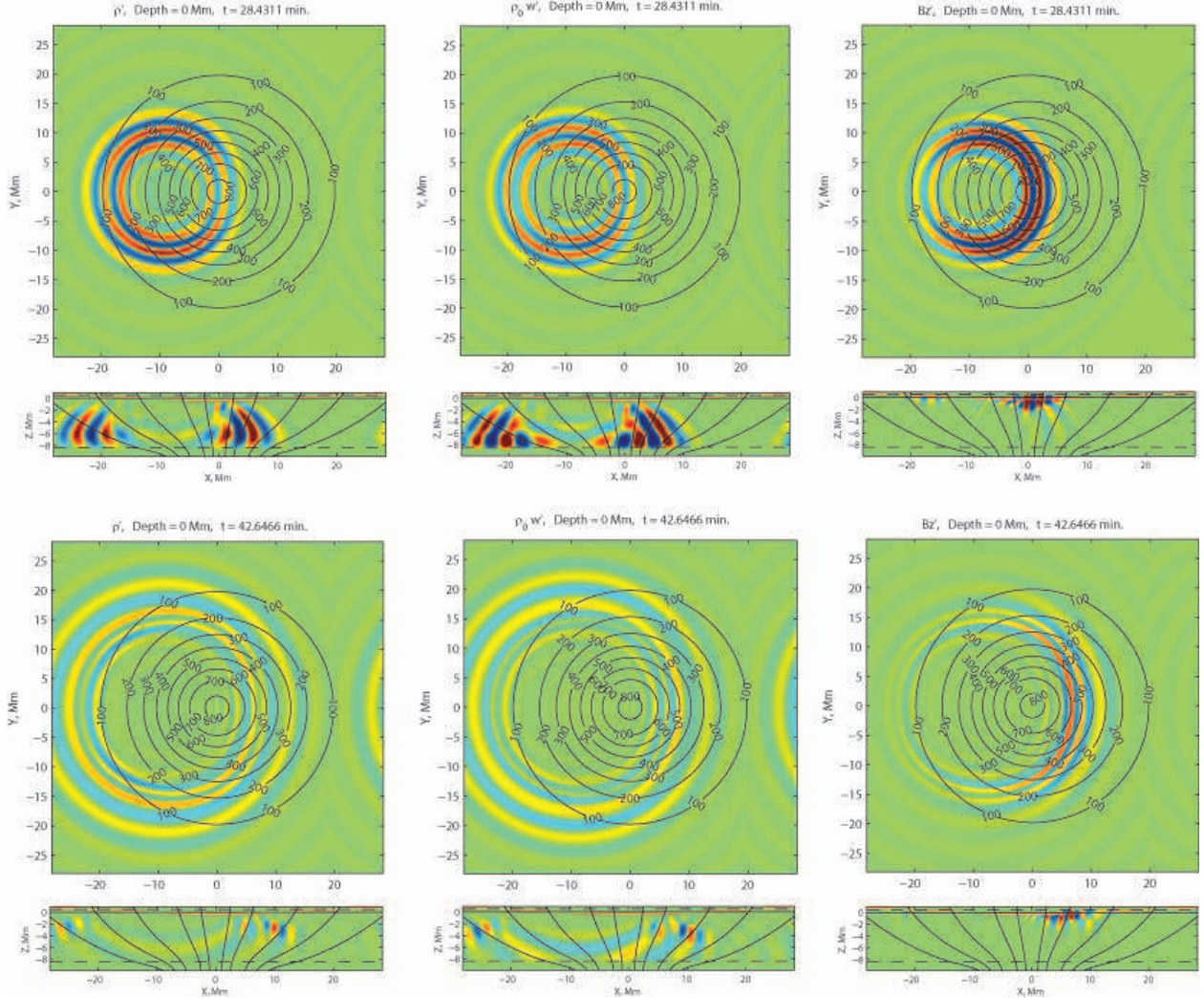


Fig. 5.— Snapshot of density ρ' (left), z -momentum $\rho_0 w'$ (middle), and B'_z (right) perturbations in the wave, propagating in the "shallow" model with the photospheric strength of the magnetic field of 0.83 kG, at moments $t=28.4$ min. (top) and $t = 42.6$ min. (bottom). The solid black horizontal lines and the red curves in the vertical cuts represent the position of the quiet photosphere and the level $\beta = 1$ respectively. Solid black curves represent the magnetic field lines.

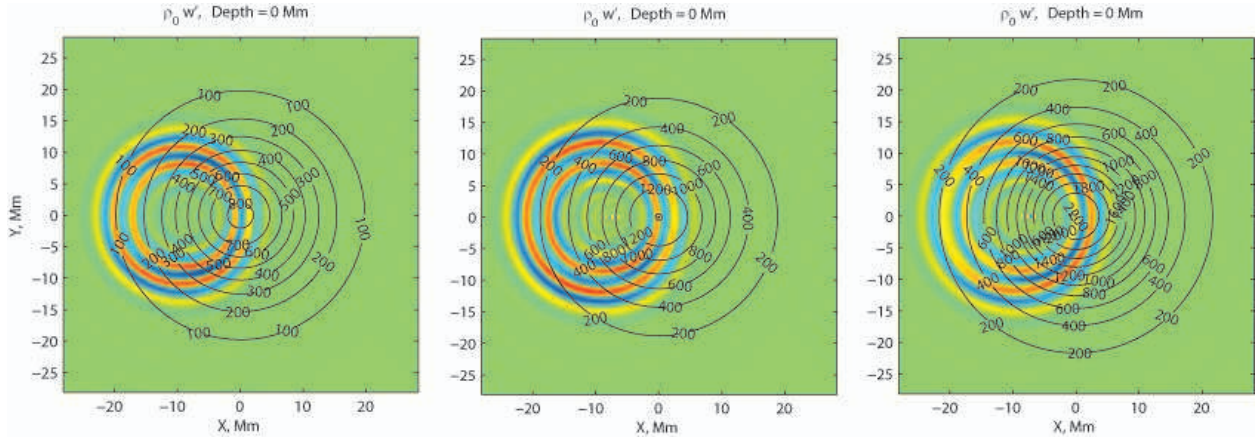


Fig. 6.— Dependence of z-momentum amplitude $\rho_0 w'$ on the photospheric strength of the magnetic field $B_{ph} = 0.83$ kG, 1.4 kG, 2.2 kG in the "shallow" models for panels a, b, and c respectively.

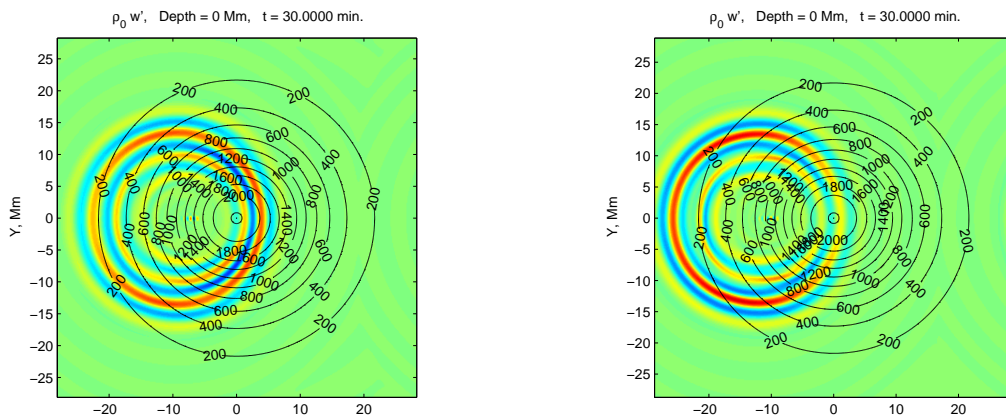


Fig. 7.— Wave fields generated by sources located at 9 Mm (left panel) and 12 Mm (right panel) from the sunspot axis in "shallow" models respectively. The photospheric strength of the magnetic field in both cases is 2.2 kG.

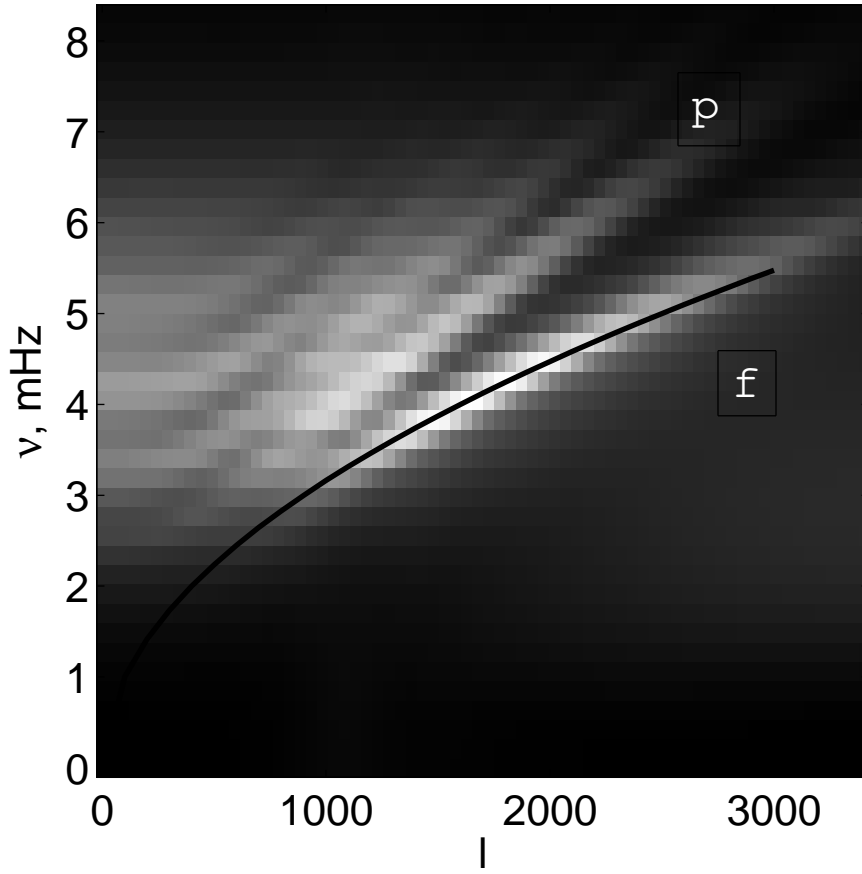


Fig. 8.— Spectrum (k - ν diagram) of the z -component of velocity for model I. The solid black curve shows the theoretical ridge of the f -mode in absence of the magnetic field.

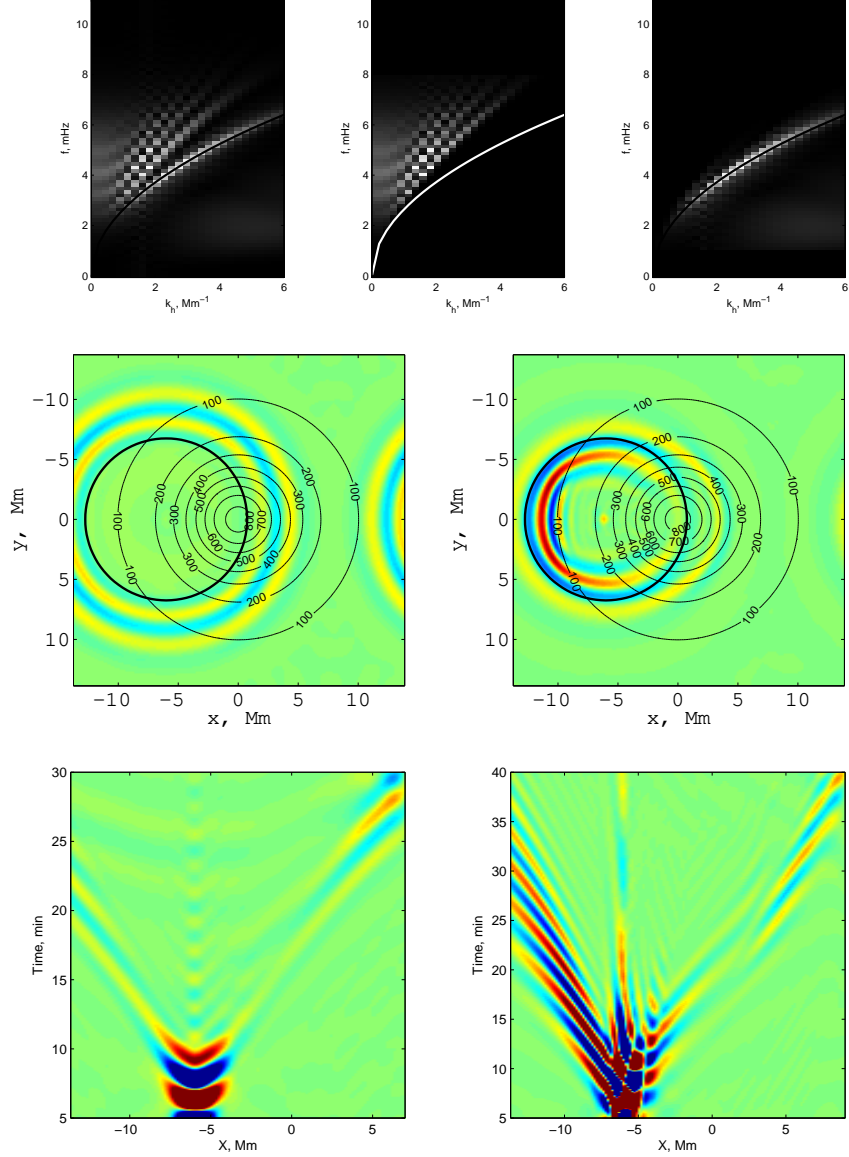


Fig. 9.— Separation of p - and f -modes by filtering. The top row represents the original and filtered k - ν diagrams. The middle row represents the corresponding maps of z -component of velocity at the moment of $t = 23$ min. for p - and f -modes respectively. The solid circle marks the inner part of the p -mode wavefront. The bottom row shows time-distance diagrams for p - (left) and f -modes (right).